SOME MEASUREMENTS IN A CONFINED TURBULENT JET

Daniel Greco Duarte*
Patrícia Rodrigues Ventura*
Juliana. B. R. Loureiro†*
Atila P. Silva Freire*

†Diretoria de Metrologia Científica, Inmetro, Duque de Caxias, 22050-050, Brasil
*PEM/COPPE/UFRJ, C.P. 68503, 21945-970, Rio de Janeiro, Brasil

Abstract. *An axisymmetric turbulent incompressible and confined jet was investigated through the laser Doppler anemometry. A special account of wall effects on jet self-preservation is given. For a confined jet the momentum flux is observed to vary with height due to contributions of reverse flow. In fact, the major effect of the return flow is to steal momentum from the jet. Results are compared with the expressions of Schneider (J. Fluid Mech., 154, 91-110, 1984) and of George (Expl Thermal FluidSci. 3,557-191, 1990). Present results show a decay in turbulent properties at that is more pronounced than that observed by other authors.*

Keywords: *Jet flow, LDA, entrainment, momentum flux.*

1. Introduction

The vast number of papers published on jets is a sure tribute to their importance in science and technology. Problems including combustion chambers, mixers, the dispersion of pollutants, the vertical take-off of airplanes, the cooling of surfaces, represent just a few of multiple applications. In addition, jets are the simplest types of turbulent shear flows that are amenable to some sort of analytical treatment. That single feature makes their understanding a particular important issue in the theory of turbulent flows.

The first theoretical treatment to a jet flow problem, the free circular jet, was given by Tollmien (1926). Using the mixing length theory of Prandtl, Tollmien was able to derive local expressions for the prediction of mean velocity profiles. Important theoretical studies soon followed on free jets including those by Schlichting (1961), Hinze (1975) and Taullbee (1989). These were complemented by some early relevant experiments carried out by Reichart (1941) and by Corrsin (1943). At the time, hot-wire anemometry was the standard measuring technique. Thus entrainment was measured indirectly through a numerical quadrature. Ricou and Spalding (1961) proposed a "porous wall" technique that instead measured entrainment directly.

In any case, the two papers that are really considered landmarks in the study of free jet flows are the papers by Bradbury (1965) and by Wygnansky and Fiedler (1969). Using the hot-wire anemometry, Bradbury (1965) showed that "self preservation on a turbulent plane jet is established at a distance of about thirty jet widths downstream of the jet nozzle and that, in the self-preserving region of the jet, the distributions of the turbulent intensities and the shear stress across the jet are very similar to those found in the plane wake". Wygnanski and Fiedler (1969) found that their circular jet was truly self-preserving after seventy diameters downstream of the nozzle. The quantities measured included mean velocities, turbulent stresses, intermittency, skewness and flatness factors, correlations, scales, low-frequency spectra and convection velocity.

All works mentioned above carried their experiments in an unbounded environment. The influence of nearly surfaces on the jet behaviour has been studied quite recently. Of course, the critical question here is: how far enough must walls be so that the flow can be considered unbounded? This problem must be particularly addressed when turbulence models are to be tested. The momentum flux is a quantity that is specially sensitive to the presence of walls. Authors including Capp and George (1982), Capp (1983), Schneider (1985), George (1990) and Hussein et al. 1994) have shown that in a bounded jet the momentum flux varies with height due to contributions of the reverse flow.

In the present work, the differences in momentum flux between a free jet and a bounded jet are studied experimentally. Through the laser Doppler anemometry, mean and fluctuating profiles are obtained at 22 different stations. The mean velocity profiles are then used to find some local properties of the flow including the entrainment coefficients and the mass and momentum fluxes. Results are compared with the expressions of Schneider (1985) and of George (1990). In particular, the present work strives at showing that a direct measurement of the entrainment velocity is possible. Furthermore, we show that the measured values agree well with those calculated through the classical theories.

2. Brief comments on the theory of jets

2.1 Integral properties and mean velocity profile

An important characteristic of a jet, be it bounded or unbounded, is its strong mixing with the surrounding fluid. This naturally results in an increase in mass flux with height, and in a spreading of velocity profile. Here we note that, for a jet, the integrated axial momentum equation has to be written differently depending whether the flow is in a bounded or in a unbounded enclosure. In the latter case, contributions by the reverse flow that is formed outside the jet must be accounted for.

The two basic integral properties of a jet are the fluxes of mass and of momentum, which can defined according by

$$\rho\mu = 2\pi \int_0^\infty \rho U r dr \tag{1}$$

$$\rho m = 2\pi \int_0^\infty \rho U^2 r dr \tag{2}$$

where U denotes the jet axial velocity at radius r from the vertical line above the source.

For a pure jet, μ becomes entirely independent of its initial value so that the jet can be treated as being defined just by the initial value of m (=M).

The mean velocity profile U self-preserving and can be represented by a Gaussian profile,

$$U(r) = U_m \exp\left[-(-r/b_{1/2})^2\right] \tag{3}$$

where U_m and $b_{1/2}$ stand respectively for the mean velocity on the centerline of the jet and for the centerline distance where mean velocity falls to half of the value on the centerline.

Turner (1986) shows by dimensional analysis that the following functional variation of U_m and of $b_{1/2}$ with M and x holds,

$$U_m = k_1 M^{1/2} x^{-1} \tag{4}$$

$$b_{1/2} = c\, x \tag{5}$$

where constant k_1 and c can be evaluated through measured profiles of mean velocity.

The value of k_1 by considering that the momentum is carried entirely by the mean flow is given by 7.5. If, however, the turbulent flux is included, this value is reduced to 6.9.

Also follows from the above results that

$$\frac{d\mu}{dx} = c_j M^{1/2} \tag{6}$$

2.2 Turbulent entrainment

A simple physical interpretation for turbulent entrainment can be as follows: It's a process characterized by the drawing of surrounding fluid across the edge of a turbulent flow. In mathematical terms this can be stated as (Morton, Taylor and Turner (1956)): the mean inflow velocity across the edge of a turbulent flow is proportional to a characteristic velocity, usually the local time-average maximum mean velocity or the mean velocity over the cross section at the level of the inflow, that is,

$$u_c = \alpha U_m. \tag{7}$$

Thus, entrainment occurs across sharply defined boundaries and this mechanism depends, in particular, on the energy balance. Turbulent flows have their energy supply on converting mean flow energy to turbulent energy by entrainment.

Through the entrainment hypothesis we can directly relate the variation in mass flux with the distance from the nozzle by considering fluid that has penetrated into the jet through its edge. Therefore, considering u_c the normal velocity across

a circular boundary, we will have from the product between the two quantities (the velocity and the area) the flux per unit of mass. In the limit, reducing the height of this area to zero, this flux can be correlated with the derivative of the mass flux with the height, Eq. 8, from where we can obtain the entrainment constant, α, from the mass flux values obtained from local velocity profiles.

$$\frac{d\mu}{dx} = 2\pi\alpha b_m U_m \tag{8}$$

2.3 The momentum flux

The momentum flux has to be treated with a lot of caution. The differences between bounded and unbounded jets are marked. In an unbounded jet the entrained mass is provided from infinity. In contrast, in a confined jet much of the entrainment is fed by a reverse flow. Since this reverse flow contributes positively to the momentum integral, is it the result of this momentum added to that in the jet that defines M. Thus, according to Hussein et al. (1994), the effect of the return flow is steal momentum from the jet. Schneider (1985), used inner and outer expansions with a multiple scale approach to proposed that the momentum flux obey Eq. 9, where C_m is a constant which depends on the angle between the jet nozzle and the wall (in our case C_m = 1) and j is 0 for two dimensional flow and 1 for axissymetrical flow. In present experiment $C_m = 1$.

$$\frac{dm}{dx} = -\frac{1}{2}\left(\frac{1}{2\pi}\frac{d\mu}{dx}\right)^2 \frac{C_m}{x^j} \tag{9}$$

The results of Schneider (1985) show that "in a turbulent jet the axial velocity decreases more rapidly than predicted by the classical boundary layer solutions and the momentum flux vanishes as the distance from the orifice tends to infinity"

Hussein et al. (1994) were particularly concerned with the effects of jet confinement. To account for wall effects, contributions by the reverse flow to momentum were computed accordingly to

$$m = 2\pi \int_0^{R_{jet}} \left(U^2 + u^2 - \frac{v^2 + w^2}{2}\right) r dr + \int_{return} U^2 dA \tag{10}$$

3. Experimental set up and instrumentation

The experimental set up is shown in Fig. 1. Details of the tank and of the jet nozzle are shown in Fig. 2.

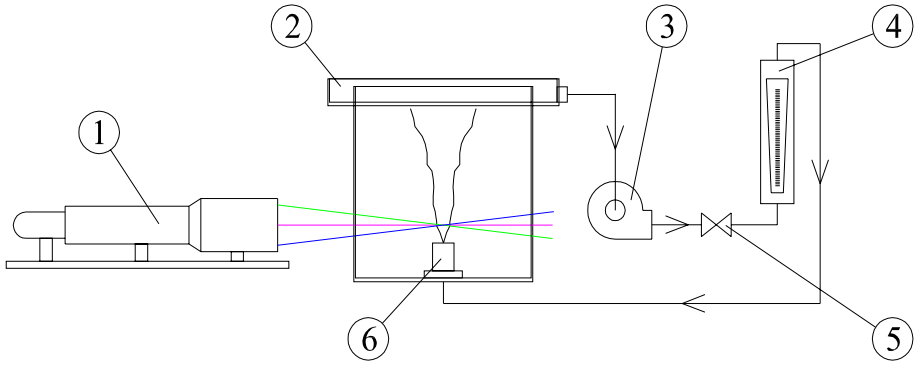

Figure 1. Experimental set up.

The tank is made of plexiglass and has dimensions of 400 x 400 x 500 millimeter; the thickness of tank walls is 8 mm. The nozzle is consisted of a small cylindrical plenum chamber of 65 mm height with an interchangeable screwed top surface and exit hole drilled at a right angle to the top surface. The present work has used a nozzle of diameter of 5 mm. The rotameter provides readings up to 700 liters per hour having a typical uncertainty of 1%.

The jet after issuing from the nozzle is collected by a tray (2) that is directly connected to a pump (3). The mass flow rate is controlled by a valve (5) and is monitored by a rotameter (4). A closed loop is granted by connecting the rotameter outflow to the nozzle.

The LDA probe is mounted on a computer-controled three-dimensional Cartesian gear system, with typical uncertainty of 0.1 mm. The whole measuring system consists of a three-component TSI laser-Doppler anemometer and a 6W Ar-ion laser source operating in multi-mode. The Ar-ion laser has multiple wavelengths. The present system separates the main

laser beam into three pairs of beams of different wavelengths, namely, a violet beam pair (476 nm), a blue beam pair (488 nm) and a green beam pair (514nm). A Bragg cell unit was used to introduce an electronic shift of around 0.6 MHz, which was adjustable via software and could be changed between each point measurement. This procedure, allowed for the resolution of the direction of the flow field and the correct measurement of near-zero mean velocities.

The system is operated in back-scatter mode using a five-beam fiber optic probe. A beam expansion ratio of 2.60 was used with a lens of 480 mm focal length in order to provide an appropriate size for the measurement volume. Supporting hardware consisted of the frequency spectrum analyzer FSA 4000, the photodetector module PDM 3500. A series of LDA biases were avoided by adjusting the strictest parameters on the data processor. For each point measured, a sample size of 20,000 values has been considered. Typical time intervals were about 60 s. The resulting uncertainty in mean velocity measurements was 0.01 m/s.

Table (1) lists the main characteristics of the laser-Doppler system used.

Table 1. Main characteristics of the three-component laser-Doppler system.

	Channel 1	Channel 2	Channel 3
Wavelength (nm)	514.5	488	476.5
Probe beam diameter (mm)	4.6	4.6	4.68
Probe beam spacing (mm)	65.0	130.0	65.0
Measurement volume diameter (μm)	75.0	70.0	68.0
Measurement volume length (mm)	1.0	0.5	1.0
Fringe spacing (μm)	3.80	1.80	3.52
Number of fringes	19	38	19

4. Experiment

Initially, extreme care was taken to ensure that the traversing system and the LDA probe were completed aligned with the tank. Next, the symmetry axis of the jet was found by considering velocity contours at 5 mm above the jet exit. The contours were taken 0.2 mm apart from each other until a distance of 10 mm away from the center was reached. A point of maximum velocity was clearly identified which allowed the characterization of the jet centerline.

The coordinate system is shown in Fig. 3.

Measurements were taken at 22 different stations, at respectively $x = 5, 10, 15, 25, 35, 40, 45, 50, 55, 60, 65, 70, 75, 80, 85, 90, 100, 110, 120, 130, 140$ e 150 mm. This distribution was observed to be good enough to distinguish the zones of (i) flow establishment (stations 5 to 35 mm) and of (ii) established flow (stations 90 to 150). In its early stages of development the jet is observed to suffer the influence of its initial conditions; this defines the region of flow establishment. On the other hand, existing results imply that some few diameters downstream of the nozzle, the jet becomes self-preserving. That is, it can be scaled by a single length and velocity scale; this defines the region of established flow. The two regions just described are shown in Fig. 4.

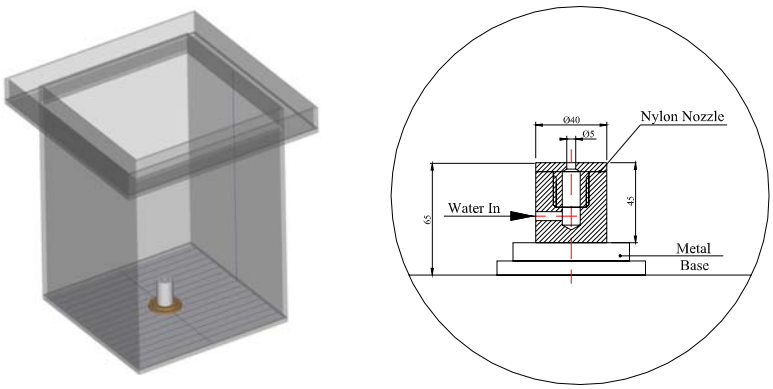

Figure 2. Details of water tank and of jet nozzle.

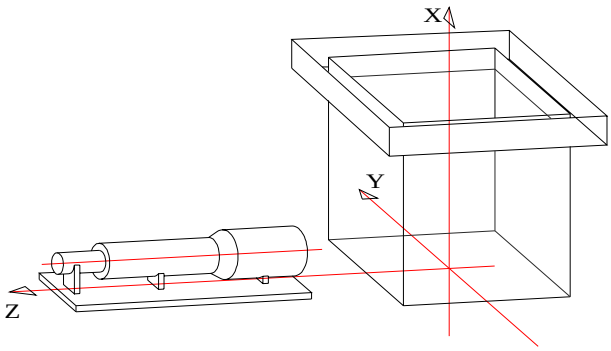

Figure 3. Coordinate system.

5. Results

5.1 Flow visualization

A flow visualization study was performed to identify the different regions of jet development. The results have already been illustrated in Fig. 4. In the near field ($x/d < 2$), instabilities and subsequent vortex rollup result in the formation of a series of vortex rings. This initial development region where structural breakdown occurs coincides with the end of the potential core and the begin of mixing transition. The rings grow as they travel downstream due to the entrainment of surrounding fluid. Depending on the vortex dynamics, two or three vortices will merge in a process normally called vortex pairing. The merging process continues until the resultant vortex is so large that its size spans the radius of the jet. The large structures then break down very suddenly into much smaller structures, of the order of half a jet diameter. This phenomenon marks the end of the transition region, normally limited by $x/d < 18$.

The fully developed turbulent jet is the flow region where self-preservation is achieved. That is, the flow region where all mean and turbulent components are in equilibrium. An equilibrium state is reached when energy production and energy dissipation of all transportable variables balance each other. Wygnansky and Fiedler (1969) remark that similarity is reached by steps. Since energy is transferred from the mean velocity to $\overline{u'^2}$ and only pressure-velocity gradient correlations transfer the energy further to other components, it is clear that first the mean velocity becomes similar which leads to a certain production of $\overline{u'^2}$, and just after an equilibrium is reached between these two quantities, an equilibrium may be achieved by the transverse turbulent components.

5.2 Velocities Profiles

The mean velocity profiles are presented so that the different regions of jet development can be easily identified. In particular, the vortex pairing and its subsequence collapse will be characterized.

The influence of nozzle conditions on the jet development can be seen in Fig. 5. The mean velocity profiles collapse in

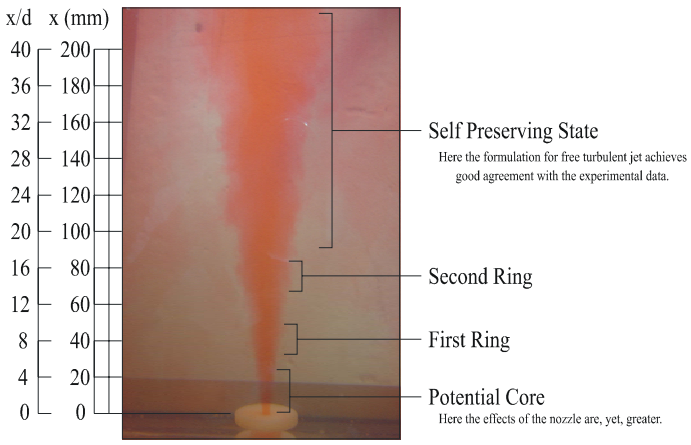

Figure 4. Flow visualization showing the distinct regions of jet development.

the range considered. However, the presence of the vortex rings can be easily seen as a great increase in $\sqrt{\overline{u'^2}}$ is observed in the region of the edge of the jet. The turbulent longitudinal intensity increases from an initial value of about 10% to a peak value of about 50% ($y/b_{1/2} > 5$). The increasing turbulent intensities are due to the growing and a subsequent radial displacement of the vortex rings

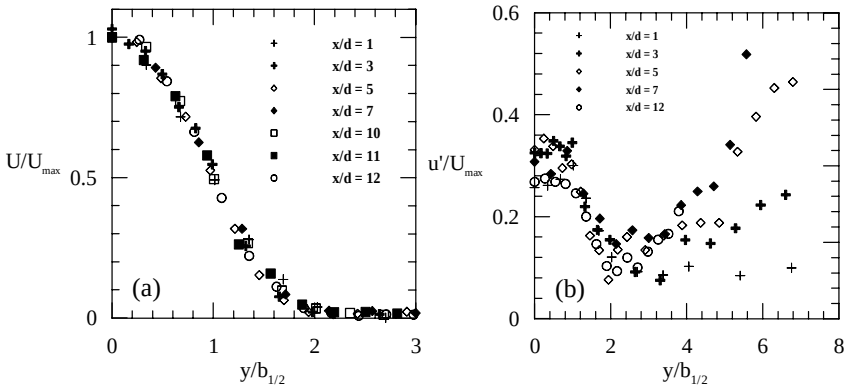

Figure 5. Mean(a) and fluctuating(b) velocities. Region of flow development ($x/d < 12$).

The transition region is characterized in Fig. 6. Throughout stations $x/d = 13$ to 17 the longitudinal intensity profiles appear to reach a stable value at the jet edge of the order of 15%. Then, suddenly turbulence levels drop sharply to very low levels. This event marks the start of the self-preserved state. This is a direct result of the collapse of the vortex rings, which move away from the main jet structure vanishing into the radial direction.

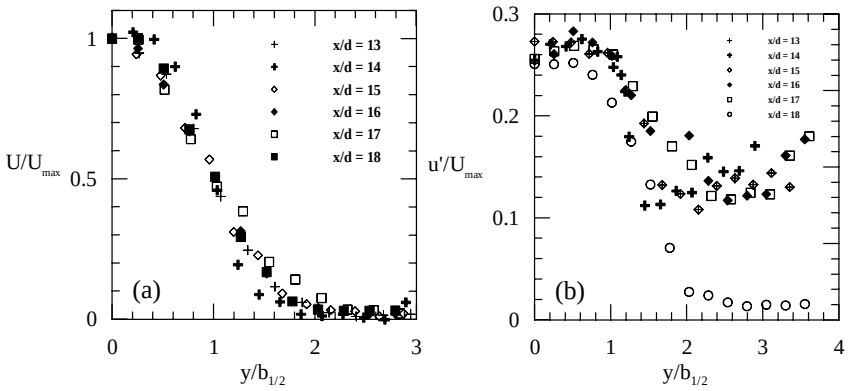

Figure 6. Mean(a) and fluctuating(b) velocities. Region of flow transition ($12 < x/d < 18$).

A self-preserved state is shown in Fig. 7. Indeed, both mean and longitudinal fluctuating velocity profiles are observed to collapse into single lines when U_{max} and $b_{1/2}$ are taken as scaling parameters.

5.3 Spreading rate, mass and momentum fluxes

The global properties of the jet, its spreading rate, mass and momentum fluxes were evaluated accordingly to the expressions presented in Section 2. The results are shown in Fig. 8.

The linear behaviour of $b_{1/2}$ and of μ is clearly illustrated. To evaluate the momentum flux, both Eqs. 9 and 10 were used. The present data do not agree well with the predicted momentum flux given by Schneider (1985). Equation 10 could not be used in its complete form for the lack of information on the behaviour of the transverse turbulent components.

5.4 Entrainment velocities

The entrained flow was evaluated by similarity arguments, by the axial variation of the mass flux and by direct measurement. Figure 9 and Tables 2 to 3 summarize the main findings. The overall results are consistent with other authors. Please note the large variation in u_e until an asymptotic value is found for $x > 0.08$ m.

Of special interest is the entrainment field of the jet. This is shown in Fig. 10. The uneven shape of the entrainment field is apparent. In fact, two peaks in the velocity entrainment profile can be seen characterizing the fluid that is drawn inside the jet from both sides. The measured positive entrainment velocity agrees well with the calculated values. The

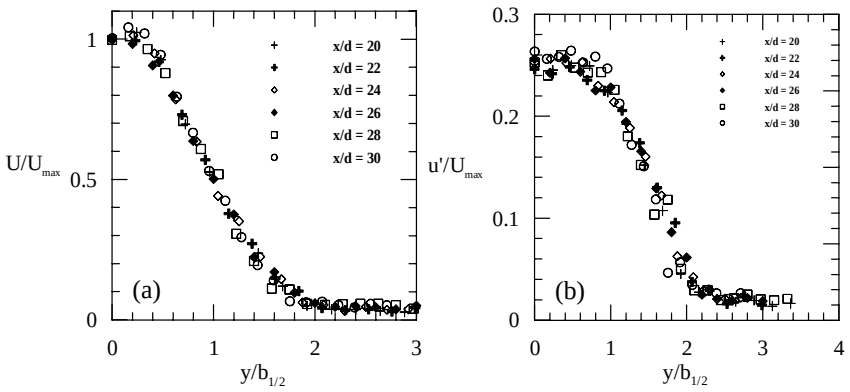

Figure 7. Mean(a) and fluctuating(b) velocities. Region of self-preservation ($20 < x/d$).

Table 2. Entrainment coefficient, α.

Author	α
Ricou and Spalding (1961)	0.08
Fischer (1979)	0.054
Hussein et al. (1994)	0.081
Present	0.058

negative velocities, on the other hand, give much lower values (Table 4).

6. Final remarks

The present work has reported some new data for a bounded jet. LDA measurements were used to find local mean and turbulent jet properties. In general a good agreement is found between the present results for the entrainment coefficients, α and C_j, and the results presented by other authors. In particular, direct measurements of the entrainment velocity were in very good agreement with results obtained through the classical equations presented in Section 2. However, results related to the momentum flux were not of the same quality. In addition to a bad agreement with Schneider's expression (Eq. 9) the overall behaviour of m clearly departs from predictions for an unbounded jet. The effects of flow confinement must then be included in the formulation of m, such as Eq. 10 proposes. Here, we have achieved our objective: to show that a direct measurement of the entrainment velocity is possible and that the obtained values agree well with those of the classical theories.

Acknowledgements. JBRL benefited from a Research Scholarship from the Brazilian National Research Council, CNPq. APSF is grateful to the Brazilian National Research Council (CNPq) for the award of a Research Fellowship (Grant No 304919/2003-9). The work was financially supported by CNPq through Grant No 472215/2003-5 and by the Rio de Janeiro Research Foundation (FAPERJ) through Grants E-26/171.198/2003 and E-26/152.368/2002.

Table 3. Entrainment constant, C_j.

Author	C_j	x/d
Albertson et al (1950)	0.28	> 8
Ricou and Spalding (1961)	0.28	> 0
Crow and Champagne (1971)	0.258	> 6
Hill (1972)	0.29	> 14
Kleis and Foss (1974)	0.27	> 6
Sforza and Mons (1978)	0.25	> 10
Fischer et al (1979)	0.25	—
Present	0.29	> 18

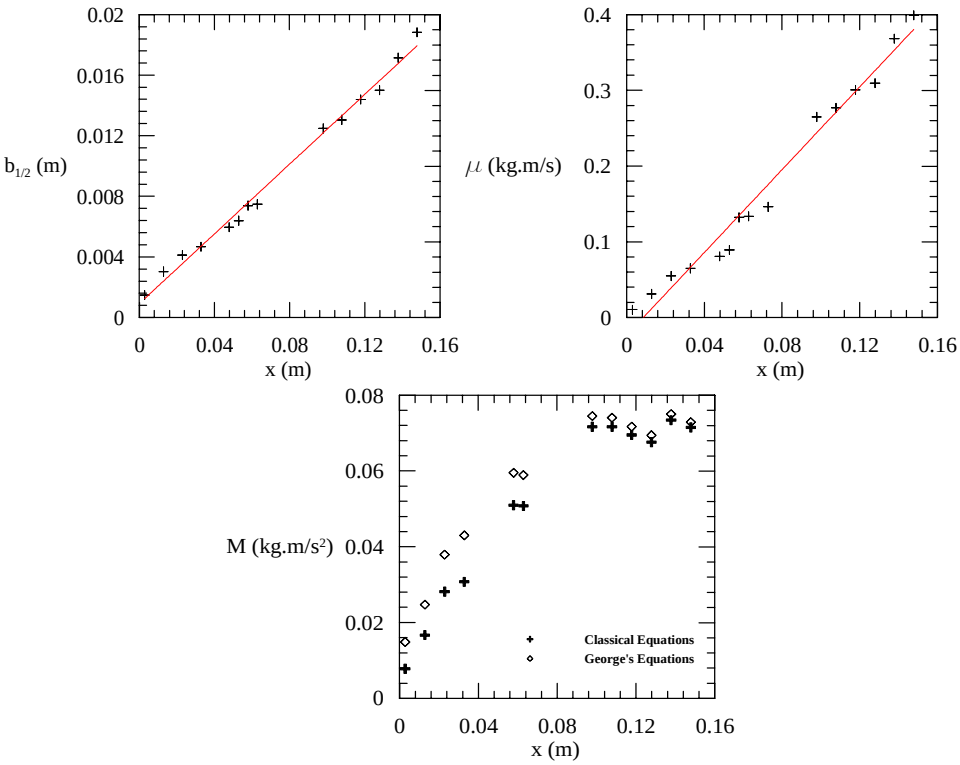

Figure 8. Spreading rate, mass and momentum fluxes.

Table 4. Entrainment velocity, u_e.

Evaluation method	u_e
Mass Flux	0.028
Direct measurement (positive-y)	0.027
Direct measurement (negative-y)	0.011

7. References

Bradbury, L.J.S. 1965 The structure of a self-preserving turbulent plane jet. J.Fluid Mech. 23, 31-64

George, W.K. 1990 Governing equations, Experiments and the Experimentalist. Expl Thermal Fluid Sci. 3,557-191

Hussein,J.H., Steven, P.,C., George, W.K. 1994. Velocity Measurements in a high-Reynolds-number,momentum-conserving, axisymmetric, turbulent jet. J.Fluid Mech. 258, 31-75

Liepmann, D., Gharib, M. 1992 The role of stream-wise vorticity in the near-field entrainment of round jets. J.Fluid Mech. 245, 643-668

Ricou, F.P. and Spalding, D.B. 1960 Measurements of entrainment by axisymmetrical turbulent jets. J.Fluid Mech. 11, 21-32

Schlichting, H. 1968 Boundary Layer theory,McGraw-Hill

Schneider, W. 1985 Decay of momentum flux in submerged jets. J.Fluid Mech. 154, 91-110

Schneider, W., Zauner, E., Bohm, H. 1987 The recirculatory flow induced by A laminar axisymmetric jet issuing from a wall.J.of Fluids Engineering. 109, 237-241

Tollmien, W.1926 Berechnung turbulenter Ausbreitungsvorgänger. ZAMM. 6, 468-472, NACA TM 1085 (1945)

Trabold,T.A., Esen ,E.B., Obot, N.T.1987 Entrainment by turbulent jets issuing from sharp-edged inlet round nozzles.J.of Fluids Engineering. 109,248-254

Turner,J.S. 1986 Turbulent Entrainment:the development of the entrainment assumption, and its application to geophysical flows. J.Fluid Mech. 173, 431-471

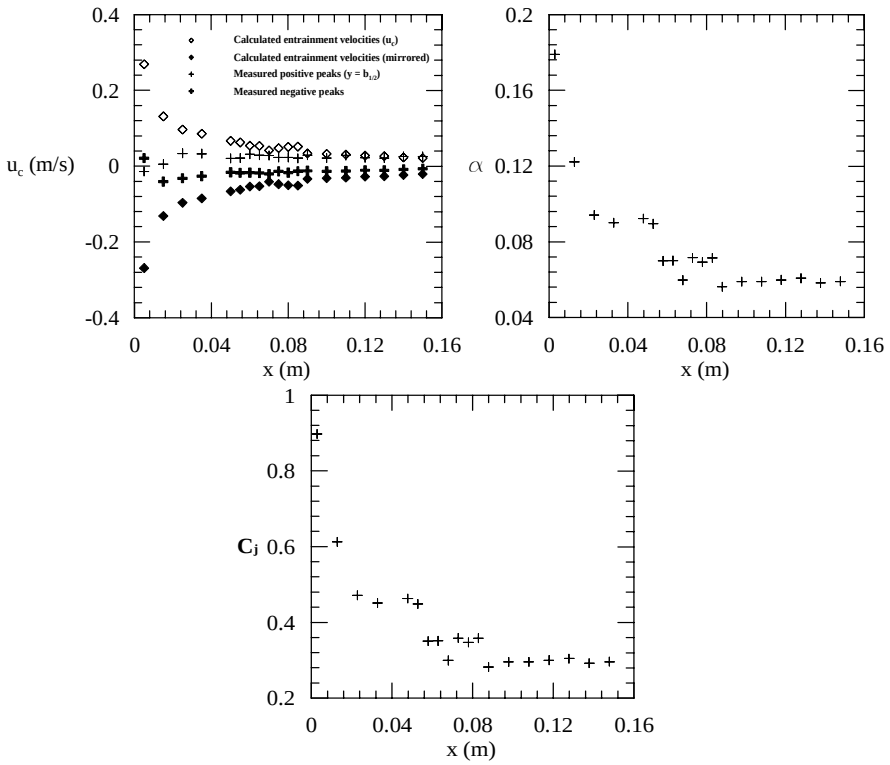

Figure 9. Behaviour of entrainment with the axial direction, including its coefficients, α and C_j.

Wygnanski, I.,Fiedler, H. 1969 Some Measurements in the self-preserving jet. J.Fluid Mech. 38, 577-612

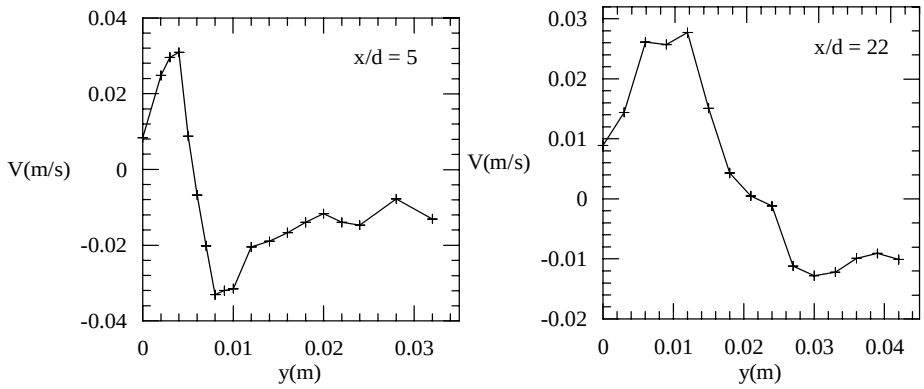

Figure 10. Radial velocity profile.